Hindawi
Advances in Civil Engineering
Volume 2019, Article ID 2465940, 13 pages
https://doi.org/10.1155/2019/2465940

Research Article

Effects of High Temperature and Cooling Pattern on the Chloride Permeability of Concrete

Zhiming Ma,[1,2] Guangzhong Ba,[1] and Zhenhua Duan[3]

[1]*College of Ocean Science and Engineering, Shanghai Maritime University, Shanghai 201306, China*
[2]*College of Civil Science and Engineering, Yangzhou University, Yangzhou 225127, China*
[3]*Department of Structural Engineering, Tongji University, Shanghai 200092, China*

Correspondence should be addressed to Guangzhong Ba; gzba@shmtu.edu.cn

Received 21 September 2018; Revised 30 November 2018; Accepted 10 December 2018; Published 13 January 2019

Academic Editor: Lukasz Sadowski

Concrete structure is frequently subjected to the fire attack, whereas the permeability of concrete with fire-damage has received little consideration. This paper aims to investigate the chloride permeability of plain concrete and recycled aggregate concrete (RAC) with fire-damage, and the effects of various cooling patterns and recuring treatment on the chloride permeability are also studied. The results manifest that the elevated temperatures result in an increase in the fire-damage and chloride permeability of concrete, and that the increase becomes more obvious with the temperature above 400°C. Attributing to the water-cooling which provides a recuring environment, the chloride permeability after water-cooling is lower than that after air-cooling when the temperature is 200°C. Whereas when the temperature is above 400°C, the chloride permeability after water-cooling becomes higher than that after air-cooling, due to an extra damage that the water-cooling produces. The recuring treatment can reduce the chloride permeability of concrete with fire-damage, and the reduction becomes more significant when the concrete suffers a serious fire-damage. Exposing to the same condition of high temperature, the addition of recycled aggregate (RA) further boosts the fire-damage and chloride permeability of concrete. Particularly, the chloride permeability increases with the increasing of RA replacement ratios, linearly, and the increased temperatures further lead to an increase in the slope of the fitting straight line.

1. Introduction

With the rapid development of construction technology, concrete is frequently subjected to the harsh environments, and the concrete structure possibly suffers a fire-damage when the fire attack happened or using the concrete as the protection materials in the furnace [1–4]. Previous studies found that the concrete's mechanical properties decreased with an increase in the elevated temperatures, and the structural safety and service life reduced correspondingly [5, 6]. The microscopic tests further revealed that the increased temperatures leaded to an increase in the development of cracks and pores in concrete [7, 8]. Exposing to the high-temperature condition, some durability experiments, such as the carbonation and freeze-thaw resistance tests, were also been conducted by the previous works, and the results demonstrated that the fire-damage resulted in a decrease in the concrete durability [9, 10], whereas the effects of fire-damage on the chloride permeability were less considered in the previous studies.

The durability deterioration frequently happens along with the water and aggressive ions penetrations into concrete. The chloride permeability, which mainly results in the steel corrosion in the reinforced concrete, is the most important indicator of the concrete durability [11–13]. In recent years, many studies on the chloride permeability have been carried out by the scholars around the world. The chloride permeability by the forces of capillary absorption, diffusion, and hydrostatic pressure was investigated, respectively, and the corresponding models were also established [14–16]. Yu et al. [17], as well as Muthulingam and Rao [18] presented the effects of mineral admixtures on the chloride permeability, and they found that appropriate content of mineral admixture reduced the chloride permeability. Zhang et al. [19] further studied the impact of freeze-thaw damage on the chloride permeability, and the results highlighted that the freeze-thaw damage enhanced

the chloride permeability. The works of Fu et al. [20] and Wang et al. [21] demonstrated that the chloride permeability increased with the increase of imposed loading damage. Ma et al. [22] further found that the water-repellent treatment can improve the resistance to chloride permeability of concrete with and without initial damage. The results above manifest that the chloride permeability is closely related to the exposure environment, the supplementary cementing materials, and concrete types [23, 24]. Moreover, the imposed damage boosts the chloride permeability significantly, which should be considered in the durability design and recovery.

Touil et al. [25] investigated the effects of temperatures (5–50°C) on the chloride permeability of saturated concrete, and the results demonstrated that the increased temperatures improved the chloride permeability. However, the effects of high temperature (above 200°C) on the chloride permeability were less considered in the previous studies. The water-cooling was frequently used in the fire extinguishing when a fire happened, whereas the laboratorial studies on the properties of concrete with fire-damage were almost conducted after air-cooling [26, 27]. Consequently, the effects of various cooling patterns on the chloride permeability should be investigated, which were less considered in the previous literatures. Furthermore, the works of Henry et al. [28, 29] and Wan et al. [30] found that the recuring treatment can recover the properties of concrete with imposed damage; for instance, an improvement in the concrete strength can be observed for concrete after recuring, whereas the related studies on the property recovery were almost focused on the microstructure and strengths and the recovery of permeability resistance received little considerations. Thus, the influence of recuring treatment on the chloride permeability of concrete with fire-damage should be studied.

Recycling the waste concrete and bricks into recycled aggregate (RA) is the most effective method of reducing the amount of construction and demolition (C&D) wastes, which meets the sustainable development of construction industry [31, 32]. The chloride permeability of recycled aggregate concrete (RAC) has been investigated by many scholars, and the results highlight that the addition of RA increases the chloride permeability [33–35]. However, the previous studies were almost conducted on the RAC without initial damage.

This paper is developed to study the influence of high temperature, cooling pattern, and the recuring treatment on the chloride permeability of plain concrete. Meanwhile, considering the wide application of RAC in the construction engineering, the chloride permeability of RAC with fire-damage has also been investigated in this paper. The elevated temperature test, the recuring treatment, and the chloride permeability test were carried out, respectively. Particularly, this paper establishes the relationship between the chloride permeability and the imposed fire-damage, which provides some necessary data for the durability design and recovery of concrete with fire-damage.

2. Materials and Experimental Details

2.1. Mixture Proportions and Concrete Specimens. Table 1 gives the mix proportion of plain concrete with the w/c ratios of 0.4 and 0.5, and the specimen is a cube with the size of 100 mm. Table 1 also shows the mix proportion of RAC, and the RA replacement ratios are 0%, 33%, 66%, and 100%, respectively. The RAC-0% specimen is also titled as the plain concrete without the addition of RA, and the RAC-100% specimen stands for all the natural coarse aggregates in concrete which are replaced by the same weight of RA.

Table 2 gives the comparison on the NA and RA properties. Due to the existence of adhered old mortar on the RA, the density parameters of RA are generally lower than those of NA, and the crushing value index of RA is about 1.14 times higher than that of NA. Particularly, the water absorption of RA is about 4.3 times higher than that of NA, and the permeability behavior of RAC is greatly affected by the high water absorption of RA. The results above highlight that the properties of RA are generally lower than those of NA. Furthermore, Figure 1 shows the particle size distribution of RA and NA. Although the particle size distribution of RA meets the requirement of Chinese standard "Pebble and crushed stone for building" (GB14685-2001), the particle size distribution of RA is generally lower than that of NA. After concrete preparing and hardening, all the specimens were placed into a curing room, where the temperature was $(20 \pm 2)^{\circ}$C and the relative humidity was above 95% for 56 days.

2.2. High-Temperature Test and Cooling Treatment. Figure 2(a) shows the sketch map of the whole testing process. The concrete specimens, after curing, were first cut into halves. Then, they were placed in the drying oven until a constant weight reached, which aims to make the concrete dry completely and prevent the concrete from spalling. After that, the high-temperature test was carried out. The targeted temperatures were 20, 200, 400, and 600°C, and the heating rate was kept at 5°C/min until the target temperature reached. The target temperature was maintained for 2 hours to induce enough fire-damage in concrete. Subsequently, all the specimens were taken out from the high-temperature furnace. For investigating the effects of cooling patterns on the chloride permeability, the one half of the specimen was cooled by air, and meanwhile, the other half of the specimen was immediately cooled by the water spraying. The air-cooling pattern refers to the specimens, after suffering high temperature, which were placed in the indoor environment with the temperature of 20°C. The water-cooling pattern stands for the specimens, after suffering high temperature, which were cooled by the water spraying until the indoor temperature reached.

The relative dynamic elastic modulus is frequently used to quantify the imposed damage of concrete. Using an ultrasonic concrete tester, the relative dynamic elastic modulus can be determined by the values of ultrasonic wave velocity or sonic time [36]. Meyers [37] proposed the relationship between the ultrasonic wave velocity and dynamic elastic modulus, as shown in Eq. (1), where the C is the ultrasonic wave velocity; E_{rd} stands for the relative dynamic elastic modulus; p presents the concrete density; and v is the Poisson's ratio. Furthermore, Zhu et al. [38] and Xv et al. [39] further gave the equation used in testing the relative

Table 1: Mix proportion of plain concrete and RAC (kg/m^3).

Specimens	Water to cement ratio	Water	Cement	Sand	Natural coarse aggregate (NA)	Recycled coarse aggregate (RA)
Plain concrete (RAC-0%)	0.4	152	380.0	580	1269	0
Plain concrete (RAC-0%)	0.5	180	360	650	1190	0
RAC-33%					797	393
RAC-66%					404	786
RAC-100%					0	1190

Table 2: Fundamental characteristics of NA and RA.

Properties		Recycled coarse aggregate (RA)	Natural coarse Aggregate (NA)
Adhesive rate of old mortar (%)		33	0
Packing density (kg/m^3)	Loose packing density	1280	1360
	Tight packing density	1440	1480
Apparent density (kg/m^3)		2530	2660
Crushing value index (%)		11	5.13
Water absorption (%)		5.3	1.0

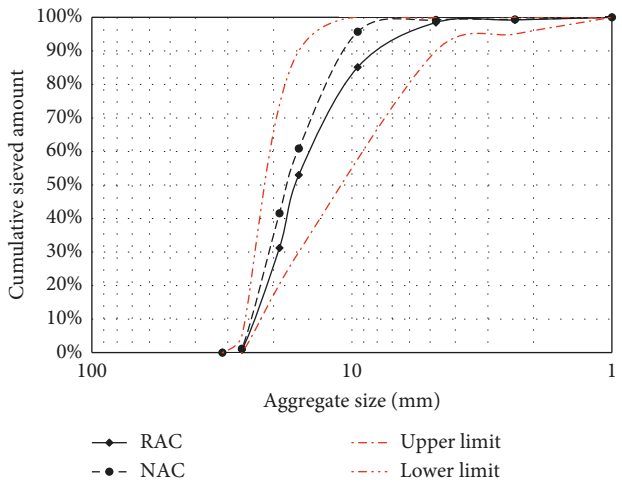

Figure 1: Particle size distribution of RA and NA.

dynamic elastic modulus of concrete with fire-damage, as shown in Eq. (2), where the E_i and E_0 are the dynamic elastic modulus of concrete with and without fire-damage; W_i and W_0 are the mass of concrete with and without fire-damage; C_i and C_0 are the ultrasonic wave velocity of concrete with and without fire-damage; and T_i and T_0 are the sonic time of concrete with and without fire-damage, and they are recorded in the ultrasonic concrete tester:

$$C = \sqrt{\frac{E_{\mathrm{rd}}(1-v)}{p(1-2v)(1+v)}}, \tag{1}$$

$$E_{\mathrm{rd}} = \frac{E_i}{E_0} = \frac{W_i}{W_0}\left(\frac{C_i}{C_0}\right)^2 = \frac{W_i}{W_0}\left(\frac{T_0}{T_I}\right)^2. \tag{2}$$

Due to the recuring treatment that provides a recovery environment and promotes the rehydration of C-S-H and $CaCO_3$, the properties of concrete with initial damage can be improved. This paper also presents the influence of recuring treatment on the chloride permeability of concrete with fire-damage. After suffering various temperatures and air-cooling, the concrete specimens were placed in the alkali solutions for 56 days. Finally, the chloride permeability tests were carried out on the concrete with fire-damage and recuring treatment.

2.3. Chloride Permeability Test. The concrete specimens after various high temperatures and cooling patterns were put into a 5% NaCl solution for 60d to conduct the chloride permeability test. After that, the specimens were dried at a drying box, and then one layer of the concrete specimen with a thickness of about 2–5 mm was milled starting from the specimen surface exposed to the NaCl solution. The chloride content of the power obtained in this way was determined by the chloride ion selective electrode (ISE), in terms of Chinese standard "Testing code of concrete for port and waterwog engineering" (JTJ 270). Figure 2(b) gives the chloride permeability test and the method of testing chloride content. Using the AgCl and calomel electrodes as the chloride ion selective electrode and the reference electrode, respectively, they were first placed in the NaCl solution for 2 h to improve their activation. Then, they were put in the NaCl solution with the concentration of 5.5×10^{-3} mol/L and 5.5×10^{-4} mol/L to build the relationship between the electric potential and the chloride concentration. Finally, the electrodes were placed in the solution in which the concrete powder was dissolved, and the chloride content per unit of concrete was obtained by the determined electric potential values.

For the concrete with saturated water, the chloride migration in concrete is mainly by the diffusion force, and it can be described by the Fick's second law, as shown in Eq. (3), where the $C(x,t)$ stands for the free chloride content at a depth x and exposure time t; C_S presents the surface chloride content; and C_o is the initial chloride content in concrete. The chloride diffusion coefficient titled D_{ap}, with the unit of 10^{-12} m^2/s, can be obtained by fitting the chloride content curves with the least-squares method:

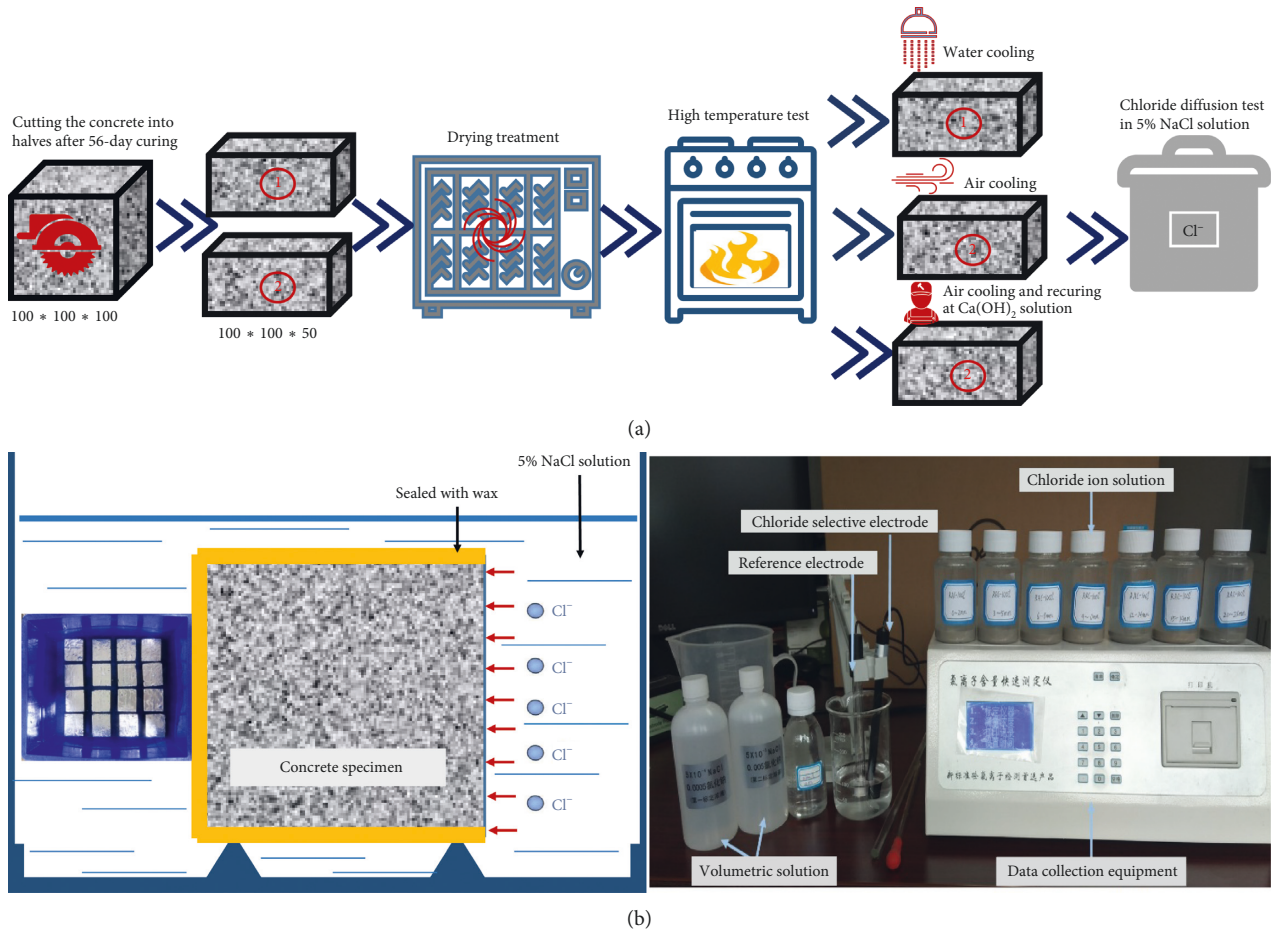

Figure 2: Testing process and methods. (a) Testing process. (b) Chloride diffusion test and chloride content determined.

$$C(x,t) = C_0 + (C_s - C_0)\left[1 - \operatorname{erf}\left(\frac{x}{2\sqrt{D_{ap} \cdot t}}\right)\right]. \quad (3)$$

3. Results and Discussion

3.1. Properties of Concrete Exposed to Various Temperatures and Cooling Patterns. The distribution of pores and cracks is closely related to the chloride permeability of concrete. Figure 3 gives the XCT and SEM images of concrete after various elevated temperatures to quantify the development of pores and cracks in concrete. Seeing from Figure 3(a), there are not the newly formed cracks and pores in concrete during the temperature below 200°C, along with the evaporation of free water and physically absorbed water in hydration products [6]. When the temperature exceeds 400°C, the $Ca(OH)_2$ begins to decompose into CaO and H_2O, as well as the microcracks in cement matrix and ITZ start to propagate and their intensity increases with temperature [6, 40]. The obvious cracks can be observed on the concrete surface after water-cooling. When the temperature is 600°C, most of the C-S-H decomposes into β–C_2S, and the carbonates begin to decompose and it is reported that this temperature generates irreversible damages [41, 42]. As shown in Figure 3(c), the obvious cracks and pores in concrete can be seen from the XCT images. In this temperature, the numbers and widths of cracks on the concrete surface after water-cooling are both higher than that after air-cooling.

Figure 4(a) shows the residual compressive strength after various temperatures and cooling patterns. The results highlight that the increased temperatures lead to the decreasing of compressive strength. For concrete with the w/c ratio of 0.5, the compressive strength after 20, 200, 400, and 600°C are 34.8, 30.1, 24.7, and 19.8 MPa, respectively. Particularly, the cooling pattern has a great impact on the residual compressive strength. With the temperature of 200°C, the residual compressive strength after water-cooling is slightly higher than that after air-cooling, because of the fact that the water-cooling treatment provides a recuring environment and the concrete properties are improved. Whereas when the suffered temperatures are above 400°C, the residual compressive strength after water-cooling becomes lower than that after air-cooling.

Zhai et al. [43] also found the similar results that the residual compressive strength after water-cooling is higher than that after air-cooling, when the suffered temperatures are below 300°C. The reason, he explained, is that the water-cooling promotes the production of hydrated calcium silicate in concrete with fire-damage, and some free water refills the

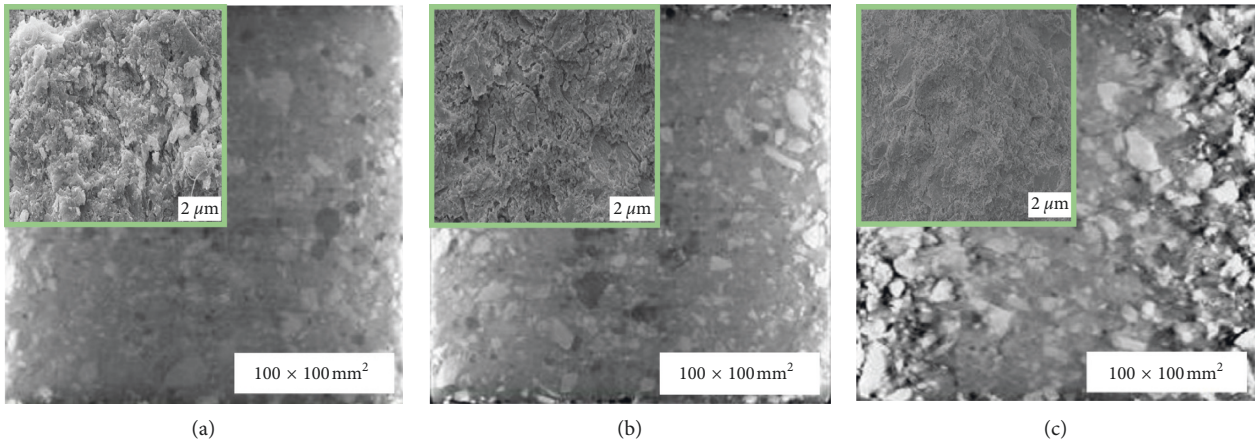

Figure 3: XCT and SEM images of concrete after various temperatures. (a) 200°C. (b) 400°C. (c) 600°C.

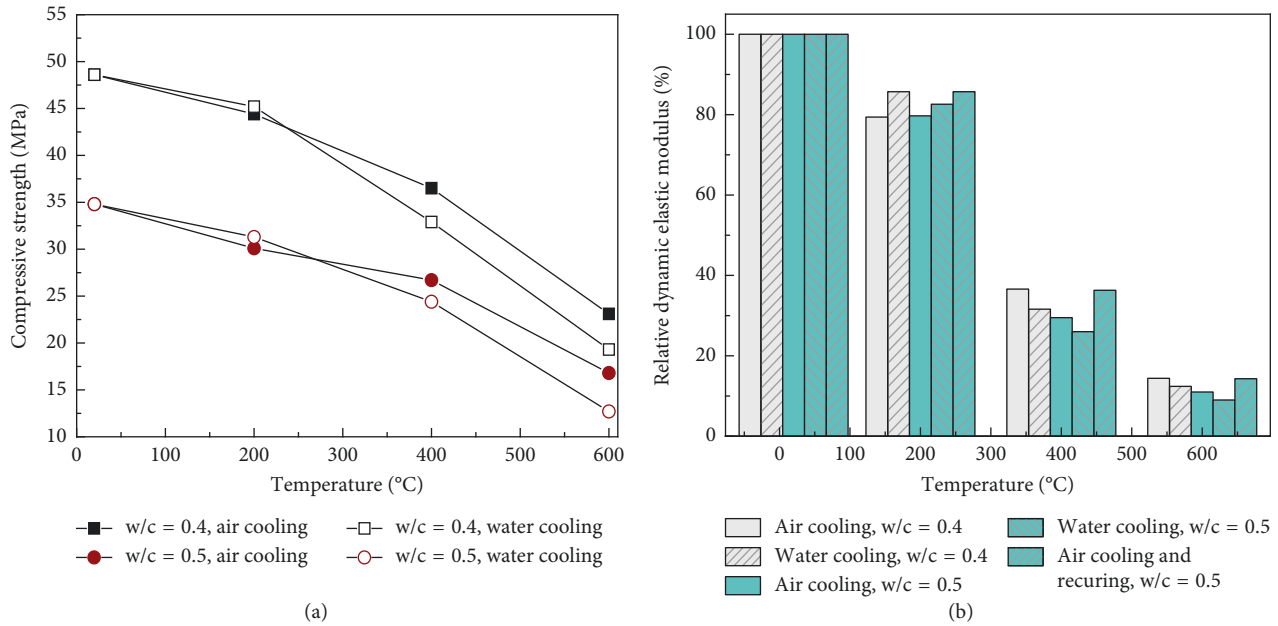

Figure 4: Properties of concrete after various temperatures and cooling patterns. (a) Residual compressive strength. (b) Relative dynamic elastic modulus.

pores in concrete. Furthermore, the unhydrated cement in concrete further produces a rehydration reaction, which resulted from the decomposition of hardened cement mortar in concrete at high temperatures [42]. Whereas when the suffered temperatures are above 400°C, the large temperature difference results in an additional damage in concrete after water-cooling, and the newly formed cracks further reduce the residual compressive strength of concrete. Thus, the residual compressive strength after water-cooling is lower than that after air-cooling, after exposing a relative high temperature (above 400°C).

Furthermore, Figure 4(b) shows the relative dynamic elastic modulus after various temperatures and cooling patterns to quantify the imposed fire-damage of concrete. The results manifest that the relative dynamic elastic modulus decreases with the increasing of temperatures and that the decrease becomes more obvious when the temperature is above 400°C. Particularly, the relative dynamic elastic modulus after water-cooling is higher than that after air-cooling when the temperature reaches 200°C, which demonstrates the concrete after water-cooling suffers a relative low fire-damage. Analyzing the reason is that the water-cooling treatment provides a recuring environment and accelerates the rehydration of cementitious materials in concrete with slight fire-damage, and some microcracks can be closed or filled with the hydration products. Whereas when the temperature is above 400°C, the relative dynamic elastic modulus after water-cooling becomes lower than that of air-cooling, and it manifests that the fire-damage after water-cooling is higher than that after air-cooling. The large temperature difference, between the cold water and the concrete with high temperature, leads to more rapid

development of cracks and pores in concrete. As a result, the relative dynamic elastic modulus reduces correspondingly.

3.2. Effects of High Temperature and Cooling Pattern on the Chloride Permeability. Chloride attack is the main reason that results in the steel corrosion in reinforced concrete, which significantly aggravates the durability degeneration and reduces the service life of concrete structure [44, 45]. Figure 5 shows the chloride content curves of concrete after various high temperatures and cooling patterns. The results show that the increased temperatures result in the growing of the maximum chloride content, and that the increase becomes more significant during the temperature above 400°C. Comparing with the results in Figures 5(a) and 5(c), as well as in Figures 5(b) and 5(d), the maximum chloride content of concrete with the low w/c ratio is lower than that with the high w/c ratio, after suffering the same temperatures and cooling patterns.

Seeing from Figure 6(a), the cooling pattern has an obvious impact on the maximum chloride content of concrete after suffering the same temperatures. When the temperature is 200°C, the maximum chloride content after water-cooling is lower than that after air-cooling. Whereas when the temperature reaches 400°C, the maximum chloride content after water-cooling becomes higher than that after air-cooling.

The chloride diffusion coefficient is closely related to the chloride penetration rate, and it can be obtained by using Fick's second law to fit the chloride content curves. As shown in Figures 5 and 6(b), the results highlight that the chloride diffusion coefficient increases with the growing of temperatures, and that the increase becomes more obvious when the temperatures are above 400°C. Seeing from Figure 5(a), the chloride diffusion coefficient after 200, 400, and 600°C are 1.39, 2.85, and 5.36 times as high as that after 20°C, respectively. This is mainly due to the increase in the pores and cracks development in concrete, which the increased temperatures lead to, and the previous studies [46] found an increase in the porosity by a factor of 1.4 between 20 and 450°C. The newly formed cracks and pores provide the more passageways for chloride penetration into concrete; thus, the chloride permeability increases. Furthermore, the chloride diffusion coefficient with the low w/c ratio is lower than that with the high w/c ratio, after suffering the same temperatures and cooling patterns.

When the temperatures are 200, 400, and 600°C, respectively, the chloride diffusion coefficient after water-cooling is about 0.94, 1.11, and 1.07 times as high as that after air-cooling, compared with the results in Figures 5(a) and 5(b). It is worth noting that the chloride diffusion coefficient after water-cooling is lower than that after air-cooling when the temperature is 200°C. This is attributed to it that the water-cooling treatment promotes the secondary hydration of the unhydrated compounds in concrete with slight fire-damage. The previous scholars [42, 47] also obtained the similar results, and they found the rehydration of the components, resulting from decomposing of concrete at high temperatures, leaded to the microstructure of concrete after water-cooling was denser than that after air-cooling. The increased density reduces the concrete's permeability; thus, the chloride permeability after water-cooling is lower than that after air-cooling when the concrete suffers a slight fire-damage. Whereas when the temperature is above 400°C, the chloride diffusion coefficient after water-cooling becomes higher than that after air-cooling. This is due to the concrete after air-cooling produced hairline cracking; however, the concrete after water-cooling experienced cracking that appeared to not only be wider but also have an increased length, 30 to 40 mm [48].

The discussions above highlight that the increased temperatures enhance the chloride permeability. Figure 7 shows the relationship between the chloride permeability and the fire-damage of concrete. The results highlight that the maximum chloride content and chloride diffusion coefficient both increase with the decreasing of relative dynamic elastic modulus and that the increase becomes more significant during the relative dynamic elastic modulus below 30%.

3.3. Effects of Recuring Treatment on the Chloride Permeability of Concrete with Fire-Damage. This part mainly investigates the effects of recuring treatment on the chloride permeability of concrete after various temperatures. Seeing from Figure 8(a), the maximum chloride content after recuring is lower than that without recuring, and the decrease in the maximum chloride content becomes more significant with the increasing of temperatures. Figure 8(b) shows the chloride diffusion coefficient of concrete with and without recuring treatment, and the results highlight that the recuring treatment reduces the chloride diffusion coefficient of concrete with fire-damage and the reduction becomes more obvious for concrete with a serious fire-damage. After 200, 400 and 600°C, the chloride diffusion coefficient with recuring treatment decreases by 0.49, 3.30, and 5.20 (10^{-12} m^2/s), respectively, compared with that without recuring treatment.

The results above manifest that the recuring treatment significantly reduces the chloride permeability of concrete with fire-damage. Under high temperature, the decomposition of hydration products results in the decrease in the concrete properties, and the decrease becomes remarkable after a relative high temperature. By the recuring treatment, sufficient water is provided for the secondary hydration reaction in concrete, and the newly formed hydration products are connected to each other. Furthermore, the morphology of concrete changes significantly after water recuring, especially the rehydration of C-S-H and $CaCO_3$ improves microstructure of concrete resulting in an increase in the concrete properties [49]. Thus, the improved concrete density reduces the chloride permeability of concrete.

3.4. Chloride Permeability of Recycled Aggregate Concrete after High Temperature. Table 3 shows the mass loss of RAC after various high temperatures. The results highlight that the mass loss increases with the growing of temperatures, and the increase becomes more remarkable during the temperature above 400°C. Such as, the mass of RAC-100% after

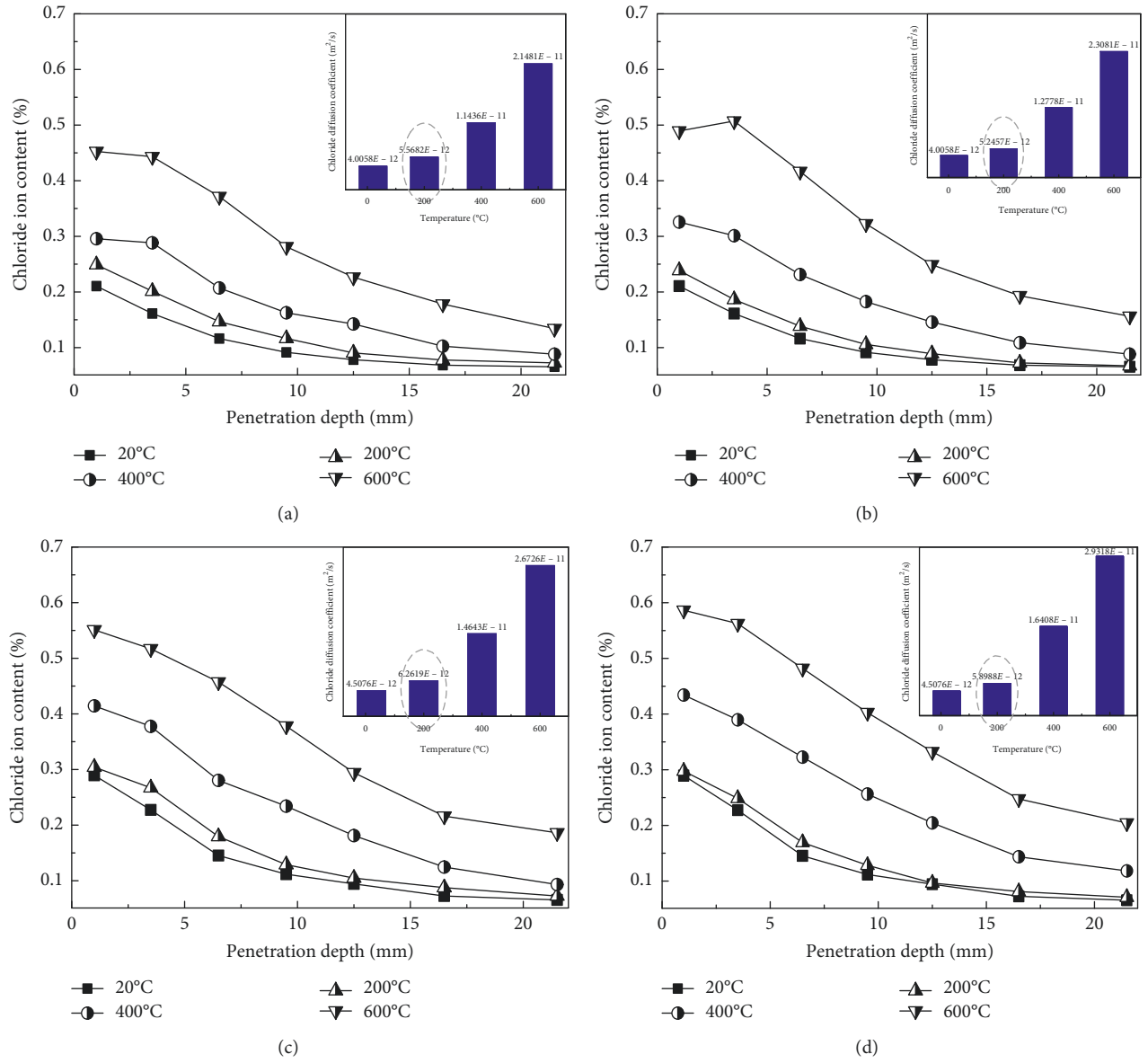

Figure 5: Chloride content curves of concrete after various high temperature and cooling patterns. (a) w/c = 0.4, air cooling. (b) w/c = 0.4, water cooling. (c) w/c = 0.5, air cooling. (d) w/c = 0.5, water cooling.

200, 400, and 600°C decreases by 1.79%, 6.16%, and 7.53%, respectively. Whereas for RAC exposed to the same temperature, the increased RA replacement ratios lead to an increase in the mass loss of concrete. Such as, the mass loss of RAC-33%, RAC-66%, and RAC-100% are 1.27, 1.42, and 1.66 times as high as that of RAC-0% with the temperature of 600°C, respectively. Table 3 also gives the relative dynamic elastic modulus to quantify the fire-damage of RAC after various temperatures. The results show that the relative dynamic elastic modulus decreases with the increase in temperatures. However, after suffering the same temperature, the relative dynamic elastic modulus reduces with the increasing of RA replacement ratios. For example, the relative dynamic elastic modulus of RAC-33%, RAC-66% and RAC-99% are 0.75, 0.55 and 0.48 times, respectively, as large as that of RAC-0% when the temperature is 400°C.

The results above manifest that the increased temperatures result in the increase in the fire-damage and the addition of RA further boosts the fire-damage of concrete. On the one hand, this is due to the addition of RA that results in the increase in the mortar content per unit volume of concrete [50]. The C-S-H, $Ca(OH)_2$, and $CaCO_3$ contents, contained in concrete, all increase with the increase of RA replacement ratios. Exposing to the high-temperature condition, the decompositions of the C-S-H, $Ca(OH)_2$ and $CaCO_3$ enhance the mass loss of concrete. On the other hand, the inferior properties of adhered old mortar and ITZ further aggravate the performance degradation of RAC under high temperature [51].

Figure 9 gives the chloride content curves of RAC after various temperatures. The results manifest that the maximum chloride content increases with the increase in temperatures. Comparing with the results in Figures 9(a)–9(d),

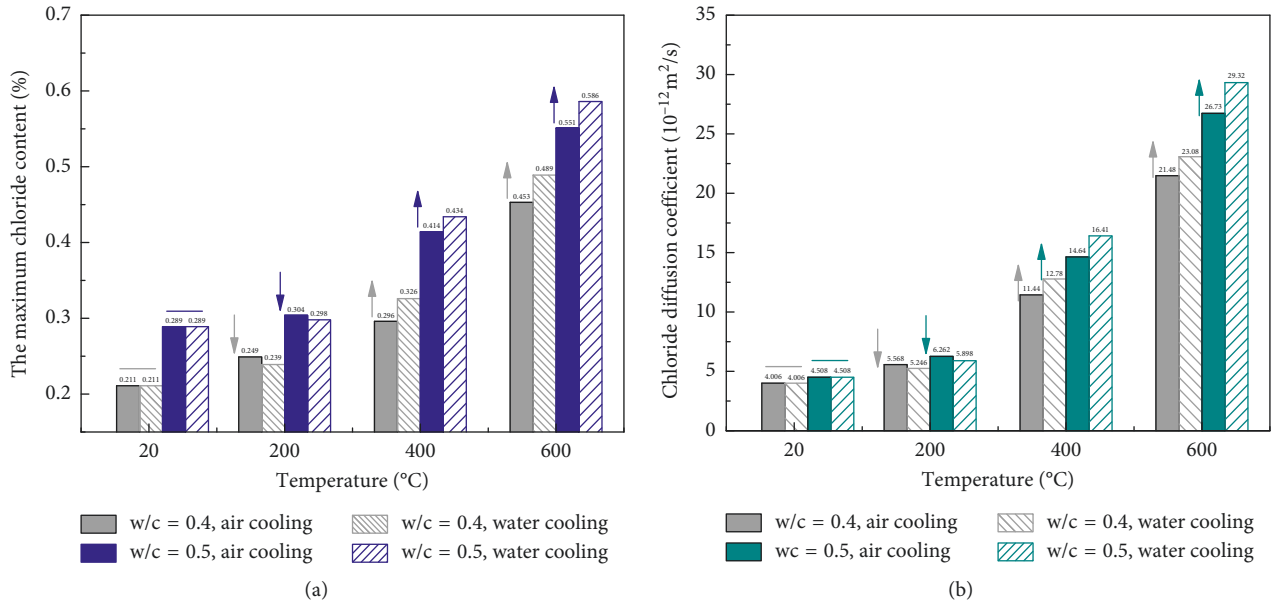

Figure 6: Chloride permeability parameters of concrete under high temperature. (a) The maximum chloride content. (b) Chloride diffusion coefficient.

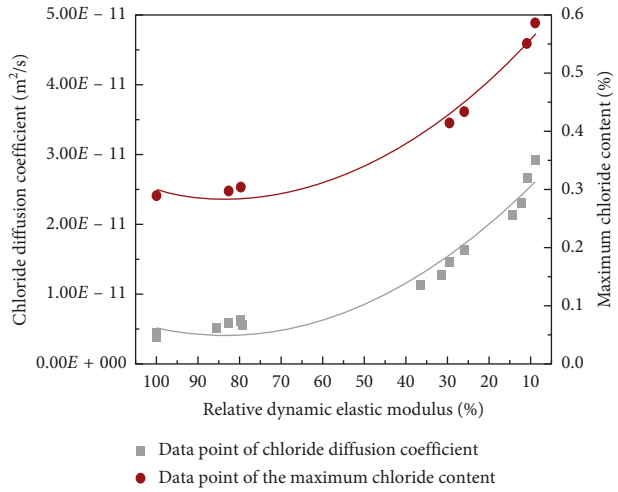

Figure 7: Relationship between the chloride permeability and imposed fire-damage.

the maximum chloride content increases with the increase in RA replacement ratios after the same temperatures, and the increase becomes more significant after a relative high temperature. Moreover, Figure 10(a) gives the relationship between the RA replacement ratios and the maximum chloride content of RAC, and the results highlight that the maximum chloride content increases linearly with the growing of RA replacement ratios after the same temperatures. Particularly, the increased temperatures result in an increase in the slope of the fitting straight line.

For RAC after the same temperatures, the chloride diffusion coefficient increases with the increase in the RA replacement ratios. For example, the chloride diffusion coefficient of RAC-33%, RAC-66%, and RAC-100% is, respectively, 1.15, 1.55, and 1.88 times as large as that of RAC-0% when the temperature reaches 600°C. Figure 10(b) further gives the relationship between the RA replacement ratios and the chloride diffusion coefficient of concrete after various temperatures. The results manifest that the chloride diffusion coefficient increases linearly with the increase in RA replacement ratios after the same temperatures. Particularly, the slope of fitting straight line increases with the growing of temperatures, which manifests that the addition of RA further enhances the chloride permeability sensibility of concrete under high temperature.

The discussions above highlight that the fire-damage enhances the chloride permeability of RAC. This is due to that the imposed damage results in an increase in the development of cracks and pores in concrete, which provides more passageways for the chloride penetrating into RAC. Attributing to the inferior properties of adhered old mortar and ITZ on RA, the addition of RA remarkably enhances

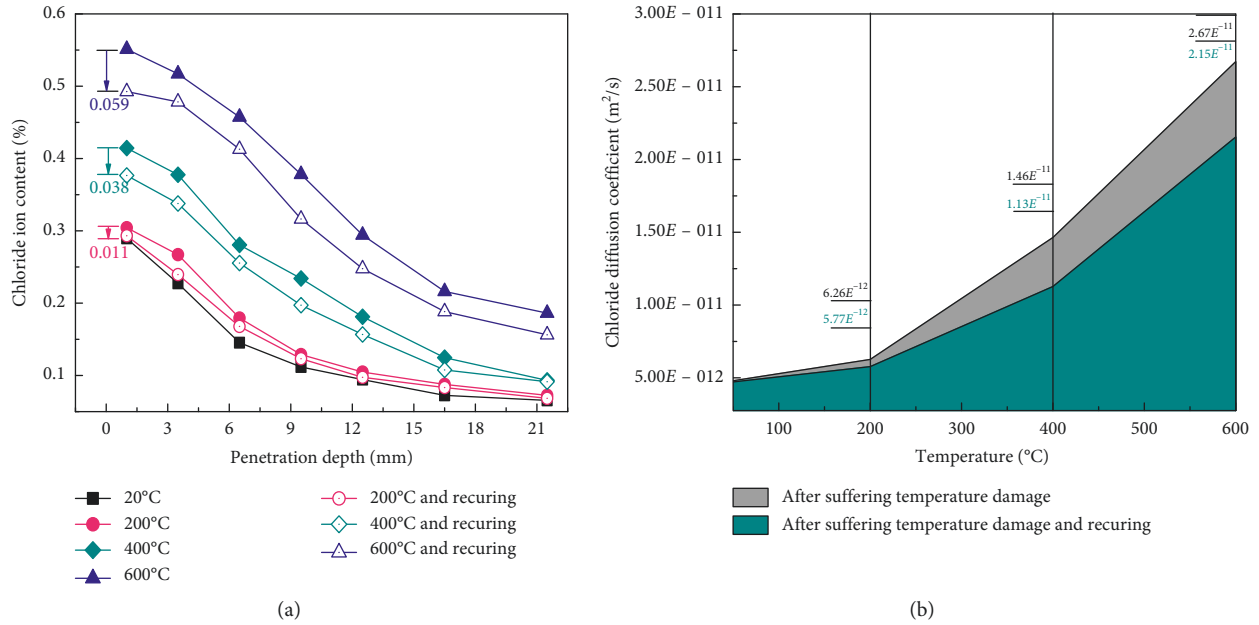

Figure 8: Chloride permeability of concrete with fire-damage and recuring treatment (w/c = 0.5). (a) Chloride content curves. (b) Chloride diffusion coefficient.

Table 3: Mass loss and relative dynamic elastic modulus of RAC after various temperatures.

Content	Specimen	20°C	200°C	400°C	600°C
E_{rd} (%)	RAC-0	100	79.7	29.5	11.0
	RAC-33	100	66.6	24.5	8.3
	RAC-66	100	58.7	16.6	6.0
	RAC-100	100	46.0	13.5	5.3
Mass loss ratio (%)	RAC-0	0	1.54	3.42	4.54
	RAC-33	0	1.59	4.04	5.77
	RAC-66	0	1.67	4.81	6.43
	RAC-100	0	1.79	6.16	7.53

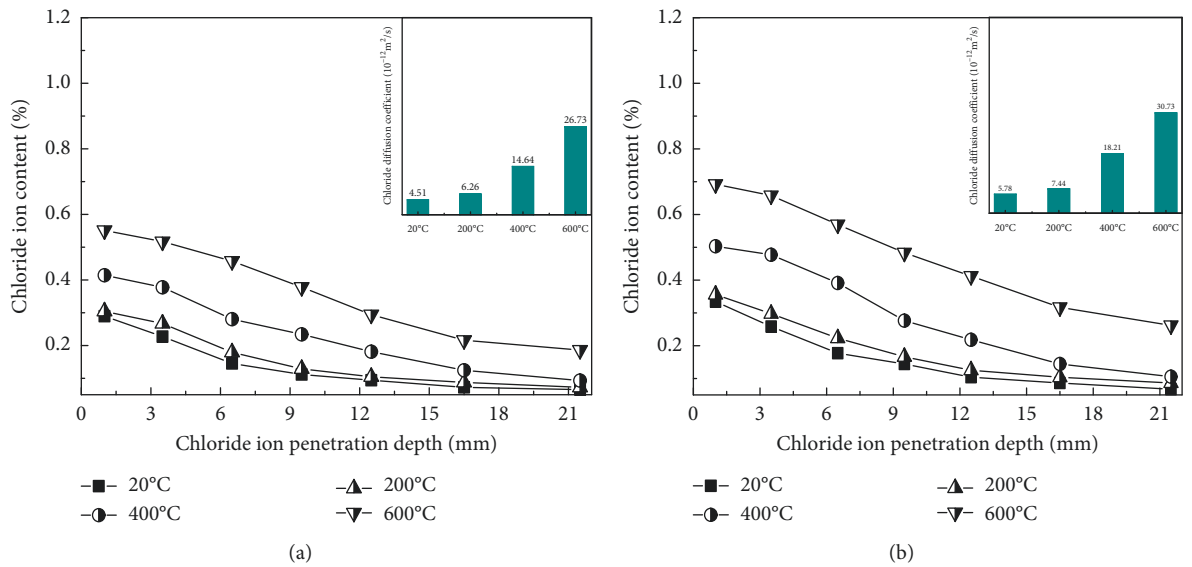

Figure 9: Continued.

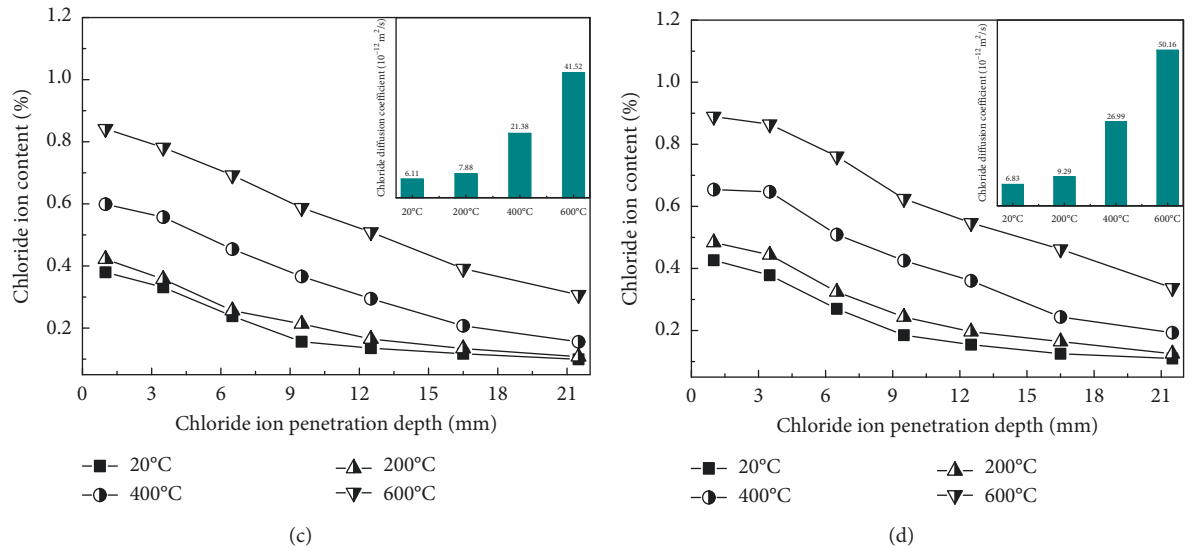

Figure 9: Chloride content curves of RAC after various high temperatures. (a) RAC-0%. (b) RAC-33%. (c) RAC-66%. (d) RAC-100%.

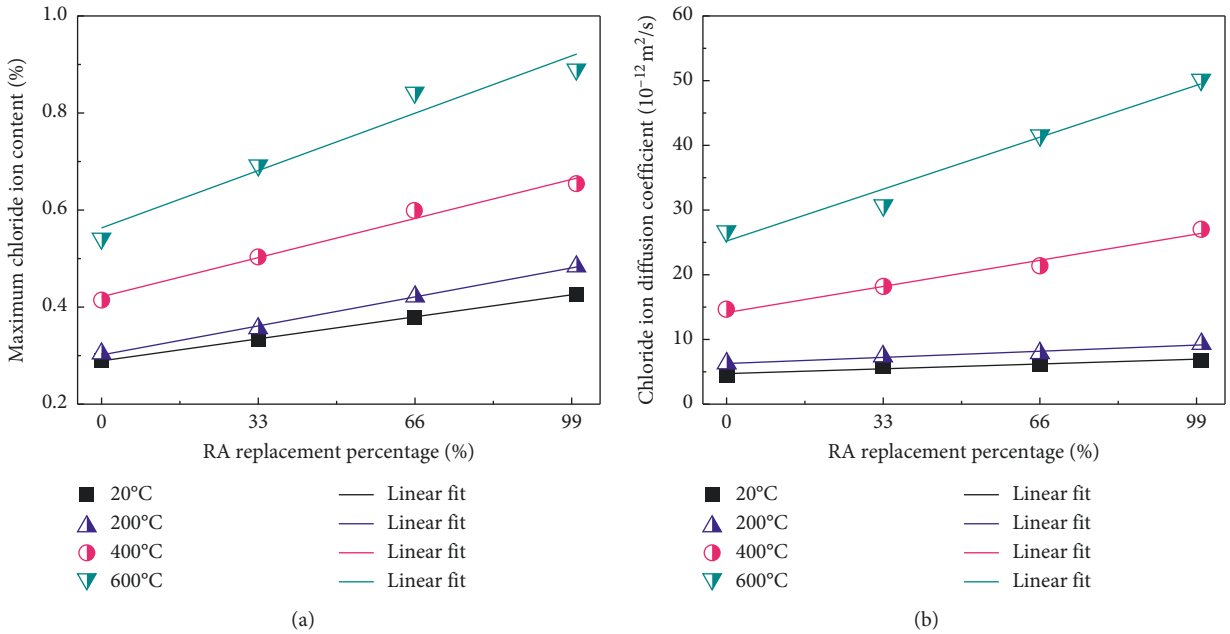

Figure 10: Relationship between the RA replacement ratios and chloride permeability of RAC under high temperature. (a) Relationship between the maximum chloride content and RA replacement ratios. (b) Relationship between the chloride diffusion coefficient and RA replacement ratios.

the fire-damage and the chloride permeability of concrete after the same temperatures. For investigating the correlation between the chloride permeability and imposed fire-damage of RAC, Figure 11(a) shows the relationship between the chloride diffusion coefficient and relative dynamic elastic modulus. When the relative dynamic elastic modulus is above 30%, the chloride diffusion coefficient increases slowly with the decrease in the relative dynamic elastic modulus, whereas the chloride diffusion coefficient significantly boosts with the further decreasing of the relative dynamic elastic modulus. Figure 11(b) gives the correlation among the RA replacement ratios, the suffered temperatures, and chloride diffusion coefficient and of RAC, which intuitively presents the chloride permeability of RAC under high-temperature condition.

Although this paper preliminary investigates the effects of high temperature and cooling pattern on the chloride permeability of concrete, there still exist some limitations needed to be studied in the further. For example, considering the mix proportion of concrete used in the actual construction, the effects of mineral admixtures should also be presented. In addition, the chloride permeability with

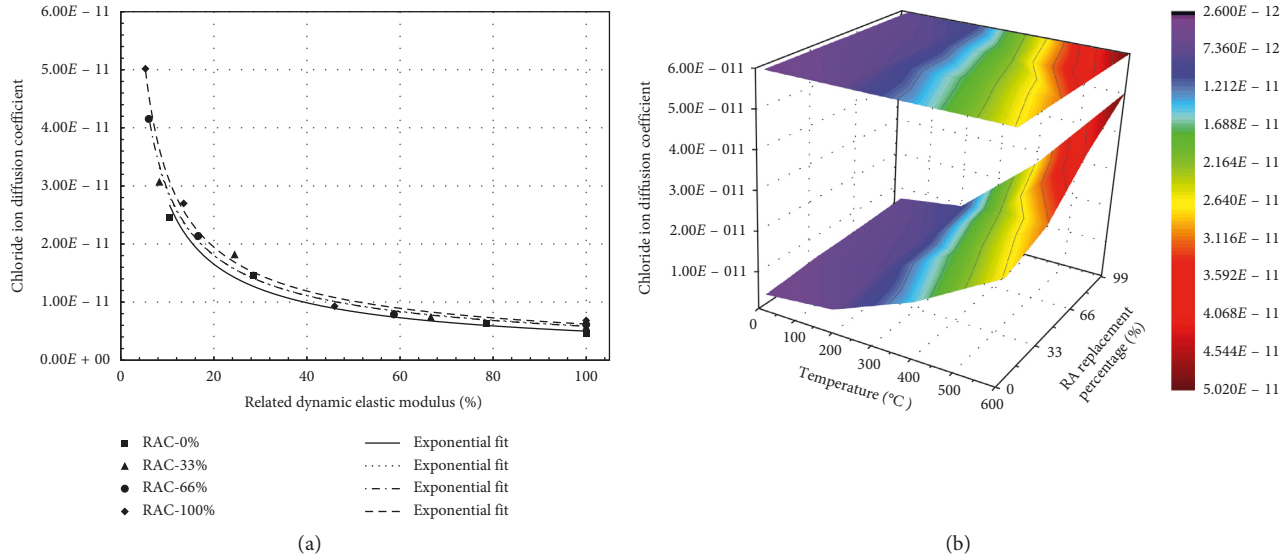

Figure 11: Correlation between the chloride permeability and the imposed fire-damage of RAC under high-temperature condition. (a) Relationship between the chloride diffusion coefficient and relative dynamic elastic modulus. (b) Correlation among the RA content, suffered temperature, and chloride diffusion coefficient.

the higher temperature (≥800°C) should be studied in the future.

4. Conclusions

Concrete is inevitably subjected to the fire attack in practice. This paper is developed to investigate the effects of high temperature and cooling pattern on the chloride permeability of concrete. Basing on the results of this experimental work, the following conclusions can be drawn.

(1) The residual strength decreases, as well as the fire-damage enhances, with the growing of temperatures, and the increase in the fire-damage becomes more obvious during the temperature above 400°C. After suffering the same temperatures, the residual strength after water-cooling is higher than that after air-cooling when the temperature reaches 200°C, whereas the residual strength after water-cooling becomes lower than that after air-cooling during the temperature above 400°C.

(2) The chloride permeability enhances with the growing of temperatures, and the increase in the chloride permeability becomes more significant when the temperature is above 400°C. The chloride permeability after water-cooling is lower than that after air-cooling with the temperature of 200°C, whereas the chloride permeability after water-cooling becomes higher than that after air-cooling when the temperature is above 400°C.

(3) The recuring treatment promotes the rehydration of C-S-H and $CaCO_3$, as well as improves the microstructure of concrete with fire-damage, which results in an increase in the concrete's dense. Thus, the chloride permeability after recuring is lower than that without recuring, and the effects of recuring treatment on the reduction of chloride permeability is more remarkable for concrete with a serious fire-damage.

(4) After suffering the same temperatures, the fire-damage and chloride permeability both increase with the increase of RA replacement ratios. The chloride permeability increases linearly with the increase in the RA content, and the increased temperatures result in an increase in the slope of the fitting straight line, which manifests that the addition of RA enhances the chloride permeability sensibility of concrete exposed to high-temperature condition.

Data Availability

The data in this manuscript were obtained through a series of tests. The related data used to support the findings of this study are available from the corresponding author upon request.

Conflicts of Interest

The authors declare that they have no conflicts of interest.

Acknowledgments

The authors gratefully acknowledge substantial support of ongoing projects under the National Natural Science Foundation of China (51708319); Natural Science Foundation of Shandong Province (ZR2017PEE015); and National Key Research and Development Program (2018YFD1101002).

References

[1] Y. K. Guruprasad and A. Ramaswamy, "Micromechanical analysis of concrete and reinforcing steel exposed to high temperature," *Construction and Building Materials*, vol. 158, pp. 761–773, 2018.

[2] Z. Ma, F. Zhu, and G. Ba, "Effects of freeze-thaw damage on the bond behavior of concrete and enhancing measures," *Construction and Building Materials*, vol. 196, pp. 375–385, 2019.

[3] H. Tanyildizi, "Prediction of the strength properties of carbon fiber-reinforced lightweight concrete exposed to the high temperature using artificial neural network and support vector machine," *Advances in Civil Engineering*, vol. 2018, Article ID 5140610, 10 pages, 2018.

[4] Z. M. Ma, Z. Q. Jin, T. J. Zhao, and Y. C. Cao, "Evaluation of high-temperature behavior of sacrificial concrete in nuclear reactor core containment structures," *ACI Materials Journal*, vol. 114, no. 6, pp. 829–838, 2017.

[5] T. Gupta, S. Chaudhary, and R. K. Sharma, "Assessment of mechanical and durability properties of concrete containing waste rubber tire as fine aggregate," *Construction and Building Materials*, vol. 73, pp. 562–574, 2014.

[6] Q. Ma, R. Guo, Z. Zhao, Z. Lin, and K. He, "Mechanical properties of concrete at high temperature-a review," *Construction and Building Materials*, vol. 93, pp. 371–383, 2015.

[7] M. Sahmaran, M. Lachemi, and V. C. Li, "Assessing mechanical properties and microstructure of fire-damaged engineered cementitious composites," *ACI Materials Journal*, vol. 107, no. 3, pp. 297–304, 2010.

[8] K. Y. Kim, T. S. Yun, and K. P. Park, "Evaluation of pore structures and cracking in cement paste exposed to elevated temperatures by X-ray computed tomography," *Cement and Concrete Research*, vol. 50, pp. 34–40, 2013.

[9] W. Wang, C. Lu, Y. Li, G. Yuan, and Q. Li, "Effects of stress and high temperature on the carbonation resistance of fly ash concrete," *Construction and Building Materials*, vol. 138, pp. 486–495, 2017.

[10] Y. Wu and B. Wu, "Residual compressive strength and freeze-thaw resistance of ordinary concrete after high temperature," *Construction and Building Materials*, vol. 54, pp. 596–604, 2014.

[11] M. Otieno, H. Beushausen, and M. Alexander, "Chloride-induced corrosion of steel in cracked concrete—Part I: experimental studies under accelerated and natural marine environments," *Cement and Concrete Research*, vol. 79, pp. 373–385, 2016.

[12] Z. M. Ma, T. J Zhao, J. Z. Xiao, and P. G. Wang, "Effect of applied loads on water and chloride penetrations of strain hardening cement-based composites," *Journal of Materials in Civil Engineering*, vol. 28, no. 9, article 04016069, 2016.

[13] Q. Wang, W. Sun, L. Guo, C. Gu, and J. Zong, "Modeling chloride diffusion coefficient of steel fiber reinforced concrete under bending load," *Advances in Civil Engineering*, vol. 2018, Article ID 3789214, 6 pages, 2018.

[14] N. S. Martys and C. F. Ferraris, "Capillary transport in mortars and concrete," *Cement and Concrete Research*, vol. 27, no. 5, pp. 747–760, 1997.

[15] Z. Ma, T. Zhao, and Y. Zhao, "Effects of hydrostatic pressure on chloride ion penetration into concrete," *Magazine of Concrete Research*, vol. 68, no. 17, pp. 877–886, 2016.

[16] W.-H. Tsao, N.-M. Huang, and M.-T. Liang, "Modelling of chloride diffusion in saturated concrete," *Computers and Concrete*, vol. 15, no. 1, pp. 127–140, 2015.

[17] Y. Yu, J. Yu, and Y. Ge, "Water and chloride permeability research on ordinary cement mortar and concrete with compound admixture and fly ash," *Construction and Building Materials*, vol. 127, pp. 556–564, 2016.

[18] S. Muthulingam and B. N. Rao, "Chloride binding and time-dependent surface chloride content models for fly ash concrete," *Frontiers of Structural and Civil Engineering*, vol. 10, no. 1, pp. 112–120, 2015.

[19] P. Zhang, F. H. Wittmann, M. Vogel, H. S. Müller, and T. Zhao, "Influence of freeze-thaw cycles on capillary absorption and chloride penetration into concrete," *Cement and Concrete Research*, vol. 100, pp. 60–67, 2017.

[20] C. Fu, H. Ye, X. Jin, D. Yan, N. Jin, and Z. Peng, "Chloride penetration into concrete damaged by uniaxial tensile fatigue loading," *Construction and Building Materials*, vol. 125, pp. 714–723, 2016.

[21] H. L. Wang, J. G. Dai, X. Y. Sun, and X. L. Zhang, "Time-dependent and stress-dependent chloride diffusivity of concrete subjected to sustained compressive loading," *Journal of Materials in Civil Engineering*, vol. 28, no. 8, pp. 1–9, 2016.

[22] Z. Ma, F. H. Wittmann, J. Xiao, and T. Zhao, "Influence of freeze-thaw cycles on properties of integral water repellent concrete," *Journal of Wuhan University of Technology-Mater. Sci. Ed.*vol. 31, no. 4, pp. 851–856, 2016.

[23] A. K. Saha and P. K. Sarker, "Durability characteristics of concrete using ferronickel slag fine aggregate and fly ash," *Magazine of Concrete Research*, vol. 70, no. 17, pp. 865–874, 2018.

[24] A. K. Saha and P. K. Sarker, "Durability of mortar incorporating ferronickel slag aggregate and supplementary cementitious materials subjected to wet–dry cycles," *International Journal of Concrete Structures and Materials*, vol. 12, no. 1, pp. 1–12, 2018.

[25] B. Touil, F. Ghomari, A. Bezzar, A. Khelidj, and S. Bonnet, "Effect of temperature on chloride diffusion in saturated concrete," *ACI Materials Journal*, vol. 114, no. 5, pp. 713–721, 2017.

[26] V. K. R. Kodur and A. Agrawal, "Effect of temperature induced bond degradation on fire response of reinforced concrete beams," *Engineering Structures*, vol. 142, pp. 98–109, 2017.

[27] J. Xiao, Z. Li, Q. Xie, and L. Shen, "Effect of strain rate on compressive behaviour of high-strength concrete after exposure to elevated temperatures," *Fire Safety Journal*, vol. 83, pp. 25–37, 2016.

[28] M. Henry, I. S. Darma, and T. Sugiyama, "Analysis of the effect of heating and re-curing on the microstructure of high-strength concrete using X-ray CT," *Construction and Building Materials*, vol. 67, pp. 37–46, 2014.

[29] M. Henry, M. Suzuki, and Y. Kato, "Behavior of fire-damaged mortar under variable re-curing conditions," *ACI Materials Journal*, vol. 108, no. 3, pp. 281–289, 2011.

[30] F. Wan, B. Sun, W. Hai, J. Wen, and H. Lu, "Experiment of concrete strength recovery after high temperature," *Concrete*, vol. 324, pp. 31–37, 2016.

[31] J. Xiao, Z. Ma, T. Sui, A. Akbarnezhad, and Z. Duan, "Mechanical properties of concrete mixed with recycled powder produced from construction and demolition waste," *Journal of Cleaner Production*, vol. 188, pp. 720–731, 2018.

[32] L. F. Jiménez, J. A. Domínguez, and R. E. Vega-Azamar, "Carbon footprint of recycled aggregate concrete," *Advances in Civil Engineering*, vol. 2018, Article ID 7949741, 6 pages, 2018.

[33] M. Bravo, J. de Brito, J. Pontes, and L. Evangelista, "Durability performance of concrete with recycled aggregates from

construction and demolition waste plants," *Construction and Building Materials*, vol. 77, pp. 357–369, 2015.

[34] R. Neves, A. Silva, J. de Brito, and R. V. Silva, "Statistical modelling of the resistance to chloride penetration in concrete with recycled aggregates," *Construction and Building Materials*, vol. 182, pp. 550–560, 2018.

[35] J. Xiao, J. Ying, V. W. Y. Tam, and I. R. Gilbert, "Test and prediction of chloride diffusion in recycled aggregate concrete," *Science China Technological Sciences*, vol. 57, no. 12, pp. 2357–2370, 2014.

[36] E. Hwang, G. Kim, G. Choe, M. Yoon, N. Gucunski, and J. Nam, "Evaluation of concrete degradation depending on heating conditions by ultrasonic pulse velocity," *Construction and Building Materials*, vol. 171, pp. 511–520, 2018.

[37] M. A. Meyers, *Dynamic Behavior of Materials*, John Wiley & Sons, Hoboken, NJ, USA, 1994.

[38] H. Y. Zhu, W. Sun, and J. Y. Jiang, "Damage evolution of sacrificial concrete subjected to elevated temperatures," *Journal of the Chinese Ceramic Society*, vol. 44, pp. 211–217, 2016.

[39] J. X. Xv, G. T. Sun, W. B. Ren, and E. X. Bai, "Ultrasonic properties of fire damage of ceramic fiber reinforced concrete," *Journal of PLA University of Science and Technology (Natural Science Edition)*, vol. 14, no. 2, pp. 213–217, 2013.

[40] A. K. Saha and P. K. Sarker, "Potential alkali silica reaction expansion mitigation of ferronickel slag aggregate by fly ash," *Structural Concrete*, vol. 19, no. 5, pp. 1376–1386, 2018.

[41] G.-F. Peng and Z.-S. Huang, "Change in microstructure of hardened cement paste subjected to elevated temperatures," *Construction and Building Materials*, vol. 22, no. 4, pp. 593–599, 2008.

[42] M. B. Karakoç, "Effect of cooling regimes on compressive strength of concrete with lightweight aggregate exposed to high temperature," *Construction and Building Materials*, vol. 41, pp. 21–25, 2013.

[43] Y. Zhai, X. Q. Ai, Z. C. Deng, and W. He, "Influence of cooling mode and high temperature on concrete compressive strength," *Journal of Hunan University (Natural Science)*, vol. 41, no. 11, pp. 74–80, 2014.

[44] Z. M. Ma, W. Li, H. X. Wu, and C. W. Cao, "Chloride permeability of concrete mixed with activity recycled powder obtained from C&D waste," *Construction and Building Materials*, vol. 199, pp. 652–663, 2019.

[45] M. Stratoura, D. R. Iaz, and E. Badogiannis, "Chloride penetration in lightweight aggregate mortars incorporating supplementary cementing materials," *Advances in Civil Engineering*, vol. 2018, Article ID 9759167, 8 pages, 2018.

[46] H. Fares, S. Remond, A. Noumowe, and A. Cousture, "High temperature behaviour of self-consolidating concrete," *Cement and Concrete Research*, vol. 40, no. 3, pp. 488–496, 2010.

[47] S. Y. N. Chan, X. Luo, and W. Sun, "Effect of high temperature and cooling regimes on the compressive strength and pore properties of high performance concrete," *Construction and Building Materials*, vol. 14, no. 5, pp. 261–266, 2000.

[48] F. U. A. Shaikh and V. Vimonsatit, "Effect of cooling methods on residual compressive strength and cracking behavior of fly ash concretes exposed at elevated temperatures," *Fire and Materials*, vol. 40, no. 2, pp. 335–350, 2014.

[49] A. H. Akca and N. Özyurt, "Effects of re-curing on microstructure of concrete after high temperature exposure," *Construction and Building Materials*, vol. 168, pp. 431–441, 2018.

[50] Q. Gao, Z. M. Ma, J. Z. Xiao, and F. A. Li, "Effects of imposed damage on the capillary water absorption of recycled aggregate concrete," *Advances in Materials Science and Engineering*, vol. 2018, Article ID 2890931, 12 pages, 2018.

[51] F. U. A. Shaikh, "Mechanical properties of concrete containing recycled coarse aggregate at and after exposure to elevated temperatures," *Structural Concrete*, vol. 19, no. 2, pp. 400–410, 2017.